

Rigorous numerical study of the Colpitts oscillator with an exponential nonlinearity

Cite as: Chaos 33, 013138 (2023); doi: 10.1063/5.0090158

Submitted: 3 March 2022 · Accepted: 27 December 2022 ·

Published Online: 26 January 2023



View Online



Export Citation



CrossMark

Zbigniew Galias^{a)}

AFFILIATIONS

Department of Electrical Engineering, AGH University of Science and Technology, al. Mickiewicza 30, 30-059 Kraków, Poland

^{a)} Author to whom correspondence should be addressed: galias@agh.edu.pl

ABSTRACT

The dynamics of the Colpitts oscillator with an exponential nonlinearity is investigated using rigorous interval arithmetic based tools. The existence of various types of periodic attractors is proved using the interval Newton method. The main results involve the chaotic case for which a trapping region for the associated return map is constructed and a rigorous lower bound for the value of the topological entropy is computed, thus proving that the system is chaotic in the topological sense. A systematic search for unstable periodic orbits embedded in the chaotic attractor is carried out and the results are used to obtain an accurate approximation of the topological entropy of the system.

Published under an exclusive license by AIP Publishing. <https://doi.org/10.1063/5.0090158>

Numerical studies suggest that for certain parameter values, the dynamics of the Colpitts oscillator is chaotic. It is, however, important to remember that this is not a mathematically proven fact. Observed chaotic trajectories may be an effect of rounding errors. It is also possible that observed trajectories are transients and the true attractor is, in fact, periodic. In this paper, we study the dynamics of the Colpitts oscillator with an exponential nonlinearity. For certain parameter values, a periodic behavior is observed in a computer simulation. In these cases, we prove that the attractor is indeed periodic. The main part of the paper is involved with the chaotic case. We prove that for certain parameter values, the Colpitts oscillator has positive topological entropy. It follows that the system supports an infinite number of periodic orbits and that chaotic trajectories exist. According to our knowledge, this is the first rigorous proof that the Colpitts oscillator is chaotic in the topological sense. A trapping region containing numerically observed trajectories is constructed from which the existence of a (possibly chaotic) attractor follows. The majority of short unstable periodic orbits embedded in the numerically observed attractor are found. The existence of these periodic orbits and their stability properties are confirmed using interval arithmetic based tools. Periods and flow times of unstable periodic orbits found are used to estimate the true value of the topological entropy of the associated return map and of the flow.

I. INTRODUCTION

In recent times, nonlinear systems, which can exhibit chaotic behavior have attracted much interest among many researchers. One of the most important features of chaotic systems is the sensitive dependence on initial conditions. In such systems, even a minor change of state variables results in significant changes in the output signal. As a consequence, predictions of system's behavior are limited to short intervals of time only. There are a lot of dynamical systems (physical, biological, etc.) that are known to be chaotic. Well known examples of electronic circuits generating chaotic trajectories include Chua's circuit¹ and the Colpitts oscillator.²

In this work, a rigorous interval arithmetic based study of the Colpitts oscillator is carried out. The Colpitts oscillator is a single-transistor device widely used for generating sinusoidal waves. Study of dynamical behaviors of the Colpitts oscillator is important for the following reasons:

1. the Colpitts oscillator is an electronic circuit used in various applications to generate sinusoidal oscillations,
2. it can operate in a wide range of frequencies (in particular, at radio frequencies) depending on the technology used,
3. it is a classic example of a simple electronic circuit capable of generating chaotic trajectories, and it is a third order system containing a single nonlinear element, and

- it has been extensively studied and various dynamical behaviors of the Colpitts oscillator have been reported in the literature,²⁻⁷
- the existence of a chaotic attractor for the Colpitts oscillator is a demanding, yet unsolved research problem.

Chaotic behavior of the Colpitts oscillator was first described in Ref. 2. The problem of stabilization of unstable periodic orbits in the chaotic Colpitts oscillator was studied in Ref. 8. Bifurcation analysis of the Colpitts oscillator was carried out in Ref. 3. Non-smooth bifurcations in a piecewise-linear model of the Colpitts oscillator were studied in Ref. 4. Chaotic behavior of the Colpitts oscillator in the ultrahigh frequency range was presented in Ref. 9. The problem of stability of oscillations in this system was discussed in Ref. 5. The dynamics and synchronization of improved Colpitts oscillators were analyzed in Ref. 10. Synchronization of chaotic oscillation in the Colpitts oscillator by a nonlinear control method was studied in Ref. 6. A single op-amp Colpitts-like chaotic circuit was investigated in Ref. 11. The dynamics of a Colpitts oscillator with a symmetrical power supply was studied in Ref. 7. Various dynamical behaviors of the Colpitts oscillator were discussed in Refs. 12 and 13. A bounded set enclosing chaotic trajectories existing in the Colpitts oscillator was constructed in Ref. 14.

However, no results concerning a rigorous analysis of a complex dynamics of this system have been reported in the literature. In particular, no one has proved before that the observed dynamics is really chaotic.

There are two types of nonlinearities used to model the dynamics of the transistor in the Colpitts oscillator: the piecewise linear and the exponential nonlinearities. In this work, we consider the latter case. The goal of this work is to carry out a thorough study of the dynamics of the Colpitts oscillator and to prove that the Colpitts oscillator is indeed chaotic. Rigorous results regarding the Colpitts oscillator are obtained using tools based on the interval arithmetic,^{15,16} where the calculations are carried out on intervals instead of standard calculations involving real numbers. The calculations are implemented in such a way that the obtained result encloses the true solution.

Interval calculations reported in this work are carried out using the CAPD library.¹⁷ Computation times are reported for a single core 3.1 GHz computer. The intervals, interval vectors, and interval matrices are denoted with bold letters, while standard (real) quantities are denoted with the usual math italic. The closed interval with the end points $\underline{x} \leq \bar{x}$ is denoted by $\mathbf{x} = [\underline{x}, \bar{x}]$. For the sake of brevity, we use a short notation to define intervals. For example, 53.76_3^4 denotes the interval $[53.763, 53.764]$. The diameter of the interval $\mathbf{x} = [\underline{x}, \bar{x}]$ is defined as $\text{Diam}(\mathbf{x}) = \bar{x} - \underline{x}$. The diameter of the interval vector $\mathbf{x} = (\mathbf{x}_1, \mathbf{x}_2, \dots, \mathbf{x}_n)$ is defined as the maximum of $\text{Diam}(\mathbf{x}_k)$ for $k = 1, 2, \dots, n$. The middle point of the interval $\mathbf{x} = [\underline{x}, \bar{x}]$ is denoted by $\text{Mid}(\mathbf{x}) = 0.5 \cdot (\underline{x} + \bar{x})$. The middle point of the interval vector $\mathbf{x} = (\mathbf{x}_1, \mathbf{x}_2, \dots, \mathbf{x}_n)$ is the vector $\text{Mid}(\mathbf{x}) = (\text{Mid}(\mathbf{x}_1), \text{Mid}(\mathbf{x}_2), \dots, \text{Mid}(\mathbf{x}_n))$.

The structure of the remaining part of this paper is as follows. Basic properties of the Colpitts oscillator are recalled and dynamical behaviors of the system for different values of parameters are reported in Sec. II. In Sec. III, the existence of periodic attractors for several values of the bifurcation parameters is proved. Rigorous

bounds for the flows times and Lyapunov exponents are calculated. The chaotic case is considered in Sec. IV. In Sec. IV A, a trapping region containing chaotic trajectories observed in simulations is constructed. The method of covering relations is used to prove that the Colpitts oscillator is chaotic in the topological sense in Sec. IV B. Sets supporting nontrivial covering relations are constructed and a positive lower bound on the topological entropy of the return map associated with the considered dynamical system is computed. A rigorous positive lower bound on the topological entropy of the flow associated with the Colpitts oscillator is found. In Sec. IV C, unstable periodic orbits embedded in a chaotic attractor are found. The method of close returns is used to locate pseudoperiodic orbits, the Newton method is applied to find approximate positions of true periodic orbits, and the interval Newton operator is used to prove their existence. The number of unstable periodic orbits and their flow times are used to obtain non-rigorous approximations of the topological entropy of the return map and of the flow.

II. COLPITTS OSCILLATOR WITH THE EXPONENTIAL NONLINEARITY

The schematic diagram of the Colpitts oscillator^{2,3} is shown in Fig. 1(a). The resonant part of the circuit consists of the capacitance divider C_1 , C_2 and the coil modeled as a series connection of the inductance L and the resistance R . The bipolar junction transistor (BJT) is biased in the active region by the voltage V_{CC} and the current source I_0 . The BJT transistor is modeled using the nonlinear resistor R_e and the current source $\alpha_F I_E$ [compare Fig. 1(b)]. We assume that the current gain α_F is equal to 1, which is equivalent to neglecting the base current. The characteristics of the nonlinear resistor R_e are given by $I_E = I_s (\exp(V_{BE}/V_T) - 1)$, where I_s is the inverse saturation current and V_T is the thermal voltage.

Following Ref. 3, let us introduce dimensionless state variables $x_1 = (V_{C1} - V_{C10})/V_T$, $x_2 = (V_{C2} - V_{C20})/V_T$, $x_3 = (I_L - I_{L0})/I_0$, where V_{C10} , V_{C20} , I_{L0} denote the operating point of the oscillator. The dynamics of the Colpitts oscillator with the exponential nonlinearity is governed by the following system of differential equations:³

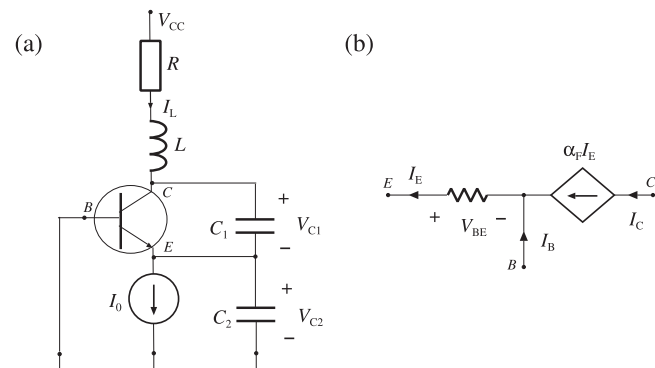


FIG. 1. (a) The Colpitts oscillator and (b) the model of the BJT transistor.

$$\begin{aligned} \dot{x}_1 &= g(Q(1 - k))^{-1}(x_3 - n(x_2)), \\ \dot{x}_2 &= g(Qk)^{-1}x_3, \\ \dot{x}_3 &= Qk(k - 1)g^{-1}(x_1 + x_2) - Q^{-1}x_3, \end{aligned} \tag{1}$$

where $n(x_2) = \exp(-x_2) - 1$, $k = C_2/(C_1 + C_2)$, g is the open loop gain of the oscillator, $Q = \omega_0 L/R$ is the quality factor, and $\omega_0 = (LC_1 C_2/(C_1 + C_2))^{-1/2}$ is the resonant frequency of the unloaded L-C circuit. For more details regarding this model, see Ref. 3.

The dynamics of the Colpitts oscillator is analyzed for the following values of dimensionless parameters: $Q \in [0.8, 1.6]$, $k = 1.5$, and $g = 4.47$. For these parameter values, the circuit has a single equilibrium point at the origin $(x_1, x_2, x_3) = (0, 0, 0)$. For $Q = 1.3$, the eigenvalues of the Jacobian matrix associated with Eq. (1) at the equilibrium $(0, 0, 0)$ are $\lambda_1 \approx -1.5522$ and $\lambda_{2,3} \approx 0.3915 \pm 1.4360i$. It follows that the equilibrium point is unstable.

Figure 2 shows trajectories of system (1) for different values of the quality factor Q . The equilibrium $(0, 0, 0)$ is plotted as a red star. For $Q = 0.88$, one can see a periodic orbit with a single turn around the equilibrium. For $Q = 0.91$, the periodic trajectory has two turns around the equilibrium and the period is approximately two times larger than for $Q = 0.88$. For $Q = 0.97$ ($Q = 0.98$), one can see periodic trajectories with four (eight) turns around the equilibrium. This is a well known cascade of period-doubling bifurcations. Further increase of the bifurcation parameter leads to a chaotic behavior ($Q = 1.3$). A periodic attractor is observed for $Q = 1.6$. This parameter value belongs to a periodic window existing within the chaotic regime.

Lyapunov exponents are a quantitative tool frequently used in the analysis of dynamical systems. They measure the average rate of the divergence or convergence of orbits starting from two closely located initial conditions. For a stable periodic orbit, the

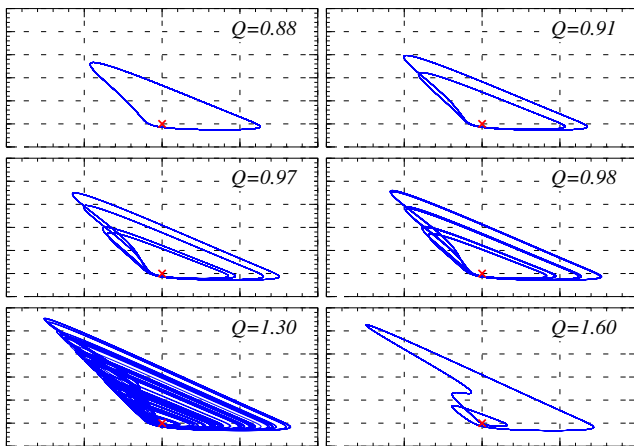


FIG. 2. Projections of steady state trajectories of the system onto the plane (x_1, x_2) for different values of the bifurcation parameter Q ; variable ranges: $x_1 \in [-100, 100]$, $x_2 \in [-10, 50]$; the red star in each plot denotes the position of the equilibrium point.

TABLE I. Lyapunov spectra for selected values of Q .

Q	λ_1	λ_2	λ_3
0.88	0	-0.016 14	-1.1268
0.91	0	-0.054 91	-1.0527
0.97	0	-0.062 67	-0.9752
0.98	0	-0.004 19	-1.0237
1.30	0.069 18	0	-0.8438
1.60	0	-0.113 01	-0.5172

largest Lyapunov exponent is zero and the other ones are negative. A bounded trajectory for which the largest Lyapunov exponent is positive is chaotic and has a property of sensitive dependence on initial conditions.^{18,19}

Table I presents the Lyapunov spectrum for the selected values of the parameter Q (compare Fig. 2). Lyapunov exponents are computed using the approach based on the Gram-Schmidt orthogonalization method.¹⁸ For $Q = 1.3$ the largest Lyapunov exponent is positive. This indicates that for this parameter value, one can expect a chaotic evolution of the system in time. For all other cases reported in Fig. 2, the largest Lyapunov exponent is zero, which suggests that the attractor is periodic. However, one should remember that values of Lyapunov exponents cannot be regarded as proofs that the attractor is chaotic (if the largest Lyapunov exponent is positive) or periodic (if the largest Lyapunov exponent is zero). The first reason is that a trajectory for which the calculations are carried out can be of a transient type, while the Lyapunov exponents should be calculated for a steady state trajectory belonging to the attractor. The second reason is that Lyapunov exponents are usually discontinuous functions of bifurcation parameters in regions where the largest Lyapunov exponent is positive. This is a consequence of the fact that frequently periodic windows densely fill a chaotic parameter region.

In the remaining part of the paper, a rigorous study of dynamical behaviors of the Colpitts oscillator for values of the bifurcation parameter reported in Table I is carried out. The dynamics is analyzed using the concept of a return map, which converts continuous time systems to discrete ones. We use the return map $P: \Sigma \mapsto \Sigma$ defined as $P(x) = \varphi(\tau(x), x)$, where $\varphi(t, x)$ denotes the trajectory of (1) starting at the initial point x and $\tau(x)$ is the return time after which the trajectory $\varphi(t, x)$ returns to $\Sigma = \{(x_1, x_2, x_3) \in \mathbb{R}^3 : x_2 = 2, \dot{x}_1 < 0\}$.

III. PERIODIC ATTRACTORS

In this section, we analyze the system behavior for cases $Q \in \{0.88, 0.91, 0.97, 0.98, 1.60\}$ in which periodic attractors are observed in simulations.

The existence of periodic attractors is proved using the interval Newton operator. For a smooth function $F: \mathbb{R}^m \rightarrow \mathbb{R}^m$, the interval vector $\mathbf{x} \subset \mathbb{R}^m$ and the point $\bar{x} \in \mathbf{x}$ the interval Newton operator is defined as

$$N(\bar{x}, \mathbf{x}) = \bar{x} - F'(\mathbf{x})^{-1}F(\bar{x}), \tag{2}$$

where $F'(\mathbf{x})$ is the interval matrix containing Jacobian matrices $F'(x)$ for all $x \in \mathbf{x}$. When evaluating the interval Newton operator, one usually selects $\bar{x} = \text{Mid}(\mathbf{x})$.

The following theorem^{15,16} can be used to prove the existence and uniqueness of zeros of F :

Theorem 1: Let \mathbf{x} be an interval vector, $\bar{\mathbf{x}} \in \mathbf{x}$ and $F: \mathbb{R}^m \rightarrow \mathbb{R}^m$ be a smooth function. Assume that $F'(\mathbf{x})$ is invertible as an interval matrix. If

$$N(\bar{\mathbf{x}}, \mathbf{x}) = \bar{\mathbf{x}} - F'(\mathbf{x})^{-1}F(\bar{\mathbf{x}}) \subset \mathbf{x}, \tag{3}$$

then map F has a unique zero in the interval vector \mathbf{x} .

Let us assume that $\bar{\mathbf{w}} = (\bar{w}_1, \bar{w}_2, \dots, \bar{w}_n)$ is the observed periodic orbit of P . To prove the existence of a true periodic orbit in a neighborhood of $\bar{\mathbf{w}}$, we construct an interval vector \mathbf{w} centered at $\bar{\mathbf{w}}$ and evaluate the interval Newton operator (2) for the map $F: \mathbb{R}^{2n} \ni \mathbf{w} \rightarrow F(\mathbf{w}) \in \mathbb{R}^{2n}$ defined as

$$F \begin{pmatrix} w_1 \\ w_2 \\ \vdots \\ w_n \end{pmatrix} = \begin{pmatrix} w_2 - P(w_1) \\ w_3 - P(w_2) \\ \vdots \\ w_1 - P(w_n) \end{pmatrix}, \tag{4}$$

where $w = (w_1, w_2, \dots, w_n)$. Map F is constructed in such a way that each period- n orbit of P is a zero of F .

To prove that \mathbf{w} contains a periodic orbit, we compute $N(\bar{\mathbf{w}}, \mathbf{w}) = \bar{\mathbf{w}} - F'(\mathbf{w})^{-1}F(\bar{\mathbf{w}})$ and verify whether $N(\bar{\mathbf{w}}, \mathbf{w}) \subset \mathbf{w}$. If this condition holds, then from Theorem 1, it follows that there exists a unique zero of F in \mathbf{w} . This zero corresponds to a period- n orbit of P and to a periodic solution of the continuous dynamical system (1).

The stability of a periodic orbit $w = (w_1, w_2, \dots, w_n)$ can be studied by computing the matrix $P'(w_n)P'(w_{n-1}) \cdots P'(w_1)$. If both eigenvalues of this matrix are smaller than 1 in the absolute value, then the orbit is stable. If at least one eigenvalue is larger than 1 in the absolute value, then the orbit is unstable.

A. A periodic attractor for $Q = 0.88$

In this case, in simulations of the return map P , one observes a stable fixed point (a period-one orbit) $w_1 \approx (53.763\ 874, 2, 3.878\ 47)$. We construct an interval vector $\mathbf{w} = \mathbf{w}_1 = (53.763^4_3, 2, 3.878^9_8) \ni w_1$ with the diameter $\text{Diam}(\mathbf{w}) = 0.001$. The evaluation of the interval Newton operator $N(\bar{\mathbf{w}}, \mathbf{w})$ with $\bar{\mathbf{w}} = \text{Mid}(\mathbf{w})$ yields $N(\bar{\mathbf{w}}, \mathbf{w}) = (53.7638^{83}_{65}, 2, 3.878\ 47^{59}_{35})$. The condition $N(\bar{\mathbf{w}}, \mathbf{w}) \subset \mathbf{w}$ is fulfilled. From Theorem 1 it follows that there exists a unique fixed point of P in \mathbf{w} .

Iterating the interval Newton operator produces an accurate bound for the position of the fixed point $\mathbf{w} = \mathbf{w}_1 = (53.763\ 873\ 674^{339}_{294}, 2, 3.878\ 474\ 716\ 9^{561}_{489})$ with the diameter $\text{Diam}(\mathbf{w}_1) \approx 4.44 \times 10^{-11}$.

The interval matrix $P'(\mathbf{w}_1)$ has eigenvalues belonging to the intervals $\mu_1 \in -0.874\ 999\ 2^{933}_{887}$ and $\mu_2 \in -8.91^{13}_{07} \times 10^{-5}$. The eigenvalues μ_1, μ_2 lie within the unit circle. It follows that the fixed point is stable. This completes the proof of the existence of a periodic attractor for $Q = 0.88$. The flow time (the length of the orbit of the continuous time system) is $t \in 8.324\ 071\ 021\ 5^2_0$.

Using the enclosures of eigenvalues μ_1, μ_2 and the enclosure of the flow time t , one can compute bounds for the non-zero Lyapunov exponents of the periodic orbit using formulas $\lambda_{2,3} = (\log |\mu_{1,2}|)/t$. This leads to the following bounds: $\lambda_2 \in -0.016\ 041\ 694^7_0$, λ_3

$\in -1.1203^{25}_{18}$. Note that the values reported in Table I are not fully consistent with the rigorous results presented here. Differences are caused by computational errors in the procedure for the calculation of Lyapunov exponents.

B. A periodic attractor for $Q = 0.91$

For $Q = 0.91$, in simulation, one observes a period-2 orbit $(w_1, w_2) \approx ((44.046\ 926, 2, 3.567\ 802), (58.375\ 567, 2, 4.269\ 907))$.

We construct an interval vector $\mathbf{w} = (\mathbf{w}_1, \mathbf{w}_2) = ((44.0469^3_2, 3.5678^1_0), (58.3755^7_6, 2, 4.2699^1_0)) \ni (w_1, w_2)$ with the diameter $\text{Diam}(\mathbf{w}) = 10^{-5}$ and verify that the condition $N(\bar{\mathbf{w}}, \mathbf{w}) \subset \mathbf{w}$ is fulfilled. The existence of a single period-2 orbit of P in \mathbf{w} follows. Iterating the interval Newton operator gives a better bound $\mathbf{w} = (\mathbf{w}_1, \mathbf{w}_2) = ((44.046\ 926\ 18^{53}_{47}, 2, 3.567\ 802\ 090^{44}_{27}), (58.375\ 566\ 608^{61}_{31}, 2, 4.269\ 907\ 173\ 5^{37}_{14}))$.

The interval matrix $P'(\mathbf{w}_2)P'(\mathbf{w}_1)$ has eigenvalues $\mu_1 \in 0.406^9_8$ and $\mu_2 \in [6 \times 10^{-9}, 6 \times 10^{-8}]$. The eigenvalues μ_1, μ_2 belong to the unit circle. It follows that the period-2 orbit is stable and that a periodic attractor exists for $Q = 0.91$. The flow time is $t \in 16.508\ 873\ 152^2_9$ and the nonzero Lyapunov exponents are $\lambda_2 \in -0.0544\ 756^8_8$ and $\lambda_3 \in -1.15^{15}_{00}$ (compare also Table I).

In this case, one can also prove the existence of a fixed point of P . Indeed, for the interval vector $\mathbf{w} = \mathbf{w}_1 = (49.936^1_0, 2, 3.863^3_2)$ with the diameter $\text{Diam}(\mathbf{w}_1) = 10^{-4}$ the condition (3) holds. It follows that \mathbf{w}_1 contains a fixed point. The eigenvalues of $P'(\mathbf{w}_1)$ are $\mu_1 \in -1.156\ 196^7_6$ and $\mu_2 \in -1.177^9_8 \times 10^{-4}$. Since $|\mu_1| > 1$ it follows that the fixed point is unstable. The flow time of the corresponding periodic orbit is $t \in 8.100\ 357\ 716\ 17^8_5$ and the nonzero Lyapunov exponents are $\lambda_1 \in 0.017\ 917\ 22^3_1$ and $\lambda_3 \in -1.1168^3_1$.

C. Periodic attractors for $Q = 0.97, Q = 0.98,$ and $Q = 1.6$

In a similar way, the existence of periodic attractors is proved for $Q = 0.97, Q = 0.98,$ and $Q = 1.6$.

For $Q = 0.97$, the existence of a periodic attractor is proved for the interval vector $\mathbf{w} = (\mathbf{w}_1, \mathbf{w}_2, \mathbf{w}_3, \mathbf{w}_4) = ((37.9507^{90}_{89}, 2, 3.533\ 33^6_5), (55.832\ 87^9_8, 2, 4.503\ 05^3_2), (33.4554^{30}_{29}, 2, 3.268\ 04^2_1), (65.905\ 22^9_8, 2, 5.008\ 25^5_7))$. The eigenvalues of $P'(\mathbf{w}_4)P'(\mathbf{w}_3)P'(\mathbf{w}_2)P'(\mathbf{w}_1)$ are $\mu_1 \in -0.125\ 779^{99}_{81}$ and $\mu_2 \in [-8.24, 8.24] \cdot 10^{-8}$.

For $Q = 0.98$, the existence of a periodic attractor is proved for the interval vector $\mathbf{w} = (\mathbf{w}_1, \mathbf{w}_2, \mathbf{w}_3, \mathbf{w}_4, \mathbf{w}_5, \mathbf{w}_6, \mathbf{w}_7, \mathbf{w}_8) = ((37.571\ 292^1_0, 2, 3.558\ 74^4_2), (54.481\ 278^1_0, 2, 4.491\ 593^2_1), (31.953\ 93^8_7, 2, 3.220\ 625^9_8), (67.359\ 534^1_0, 2, 5.145\ 377^9_8), (38.340\ 684^3_2, 2, 3.603\ 7608^4_2), (52.782\ 57^3_1, 2, 4.401\ 930^1_0), (32.390\ 48^9_8, 2, 3.246\ 9852^3_1), (66.360\ 18^1_0, 2, 5.096\ 156^5_7))$. The eigenvalues of $P'(\mathbf{w}_8)P'(\mathbf{w}_7) \cdots P'(\mathbf{w}_1)$ are $\mu_1 \in -0.758\ 43^{85}_{30}$ and $\mu_2 \in [-2.72, 2.72] \cdot 10^{-6}$.

For $Q = 1.6$, the existence of a periodic attractor is proved for the interval vector $\mathbf{w} = (\mathbf{w}_1, \mathbf{w}_2) = ((7.224\ 76^7_6, 2, 2.841\ 411^1_0), (61.621\ 80^8_7, 2, 8.905\ 506^5_5))$. The eigenvalues of $P'(\mathbf{w}_2)P'(\mathbf{w}_1)$ are $\mu_1 \in -0.112\ 37^{39}_{01}$ and $\mu_2 \in -4.71^{33}_{33} \times 10^{-5}$.

In all cases, eigenvalues of the matrix $P'(\mathbf{w}_p)P'(\mathbf{w}_{p-1}) \cdots P'(\mathbf{w}_1)$, where p denotes the period of the orbit, lie within the unit circle. It follows that the corresponding periodic orbits are stable and, hence, that these periodic orbits are attractors. Parameters of periodic attractor are collected in Table II.

TABLE II. Rigorous bounds for the flow times t and Lyapunov exponents $\lambda_1 > \lambda_2 > \lambda_3$ for periodic attractors. For $Q = 0.91$, we also report the parameters of the unstable periodic orbit.

Q	t	λ_1	λ_2	λ_3
0.88	8.324 071 021 5 ₀ ²	0	-0.016 041 694 ₀ ⁷	-1.1203 ₁ ³
0.91	16.508 873 152 ₇ ⁹	0	-0.054 475 6 ₆ ⁸	-1 ₀₀ ¹⁵
0.91	8.100 357 716 17 ₂ ⁸	0.017 917 22 ₁ ³	0	-1.1168 ₁ ³
0.97	33.302 314 566 ₄ ⁴	0	-0.062 254 ₅ ⁷	< -0.4899
0.98	66.484 668 3 ₂ ⁴	0	-0.004 158 ₇ ⁹	< -0.1929
1.60	19.503 979 910 ₆ ⁸	0	-0.112 07 ₅ ⁸	-0.51 ₀ ⁶

IV. CHAOTIC CASE

In this section, we analyze the case $Q = 1.3$ for which a chaotic behavior is observed in simulations (compare Fig. 2). We construct a trapping region for the return map, thus proving the existence of an attractor. We prove that the system supports an infinite number of periodic orbits and that the Colpitts oscillator is chaotic in the topological sense. We also carry out a systematic search for unstable periodic orbits embedded in the attractor and estimate the true value of the topological entropy of the return map.

A. The existence of an attractor

The existence of an attractor is proved by constructing a trapping region candidate T enclosing a computer-generated trajectory of the return map P and showing using methods based on the interval arithmetic that the set T is indeed a trapping region.

A trapping region T for the map P is defined as a set in the domain of the map which is mapped into itself, i.e., $P(T) \subset T$. The polygon T being a trapping region candidate for the return map P is shown in Fig. 3. The definition of the polygon T is given in the Appendix. To prove that T is a trapping region we use the generalized bisection method. First, we cover the set T by boxes \mathbf{x}_k

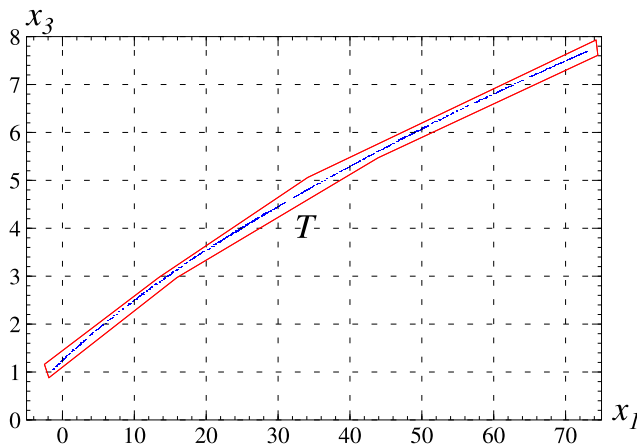


FIG. 3. The border of the trapping region candidate T (red) enclosing a trajectory of P (blue).

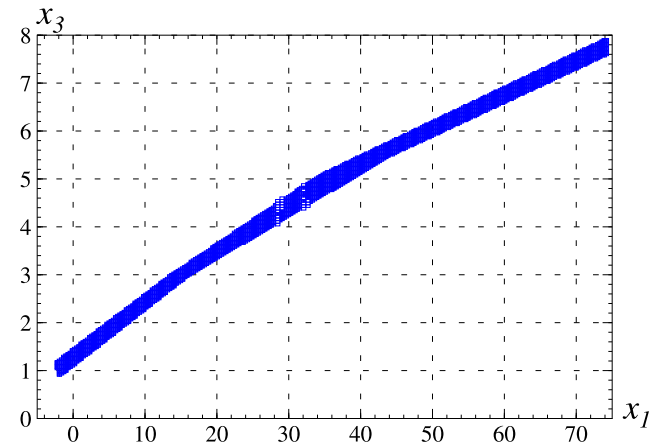


FIG. 4. Covering of the interior of T composed of 2980 boxes for the proof that the return map P is well defined on T .

(two-dimensional interval vectors) of a specified size, for each box \mathbf{x}_k find an enclosure \mathbf{y}_k of the image $P(\mathbf{x}_k)$ and verify the condition $\mathbf{y}_k \subset T$. If this condition does not hold, we split \mathbf{x}_k into smaller boxes, skip boxes having empty intersection with T (if any), and repeat the computations. Applying this procedure to the candidate set T results in a covering composed of 96 939 boxes \mathbf{x}_k with the diameters above 0.0375. For each box, it is verified that $P(\mathbf{x}_k) \subset T$, which completes the proof that T is a trapping region for P . The computer assisted proof takes approximately 530 s.

It is possible to shorten the computation time using the property of uniqueness of solutions of (1). From this property, it follows that it is sufficient to prove that (i) the condition $P(x) \subset T$ holds for each x from the border of T and (ii) the return map P is well defined on T . In both parts of the proof, the generalized bisection approach can be used. During the proof, the border of T is covered by 3599 boxes \mathbf{x}_k and the condition $P(\mathbf{x}_k) \subset T$ is verified. The interior of T is covered by 2980 boxes \mathbf{x}_k for which enclosures of images $P(\mathbf{x}_k)$ are found. In this way, it is confirmed that the return map P is well defined on T . Covering of the interior of T is shown in Fig. 4. The whole proof takes approximately 39 s (19 s for the border and 20 s for the interior). The computation time is significantly shorter than in the first version.

From the fact that T is a trapping region, it follows that T contains an attractor or multiple attractors.

B. Positive topological entropy

In this section, we show that the return map P associated with the Colpitts oscillator is chaotic in the topological sense, i.e., its topological entropy is positive. The method of covering relations is used to compute a rigorous lower bound of the topological entropy of the return map.

Topological entropy¹⁹ of a discrete time dynamical system characterizes mixing of points of the phase space. It is said that a discrete or continuous dynamical system is *chaotic in the topological sense* if its topological entropy is positive.¹⁹

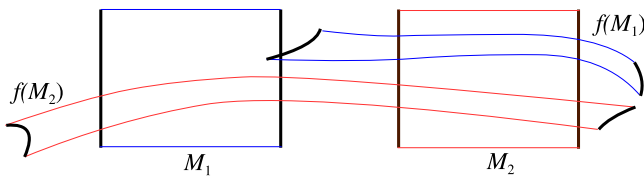


FIG. 5. Example covering relations. M_1 f -covers M_2 , M_2 f -covers M_1 and M_2 . Vertical edges and their images are plotted in black.

Covering relations^{20,21} are a topological tool, which can be used for proving the existence of periodic orbits and complex symbolic dynamics. Let us briefly describe this idea in a two-dimensional setting. Let $f: \mathbb{R}^2 \mapsto \mathbb{R}^2$ be a continuous map. Let $M_1, M_2, \dots, M_k \subset \mathbb{R}^2$ be pairwise disjoint sets. Each set M_i is a topological rectangle with predefined horizontal and vertical edges. We say that M_i f -covers M_j if and only if the images of vertical edges of M_i lie geometrically on the opposite sides of the rectangle M_j and the image $P(M_i)$ is enclosed in the interior of the topological stripe defined by the horizontal edges of M_j (the image $P(M_i)$ has an empty intersection with the horizontal edges of M_j). Example covering relations are shown in Fig. 5.

The existence of covering relations involving the map f can be used to obtain a lower bound for the topological entropy $h(f)$ of f (compare Refs. 19 and 22). Assume that there exist certain covering relations regarding the map f and the sets M_1, M_2, \dots, M_k . The transition matrix $A \in \mathbb{R}^{k \times k}$ is defined in the following way: $A_{ij} = 1$ if M_i f -covers M_j , and $A_{ij} = 0$ otherwise. Then, the topological entropy $h(f)$ is not less than the logarithm of the dominant eigenvalue of the transition matrix A .

In the first step of the computer assisted proof that P is chaotic in the topological sense, the candidate topological rectangles M_1, M_2, \dots, M_5 are found (see Fig. 6). Definitions of the sets M_i are given in the Appendix. Finding sets with positive topological entropy is

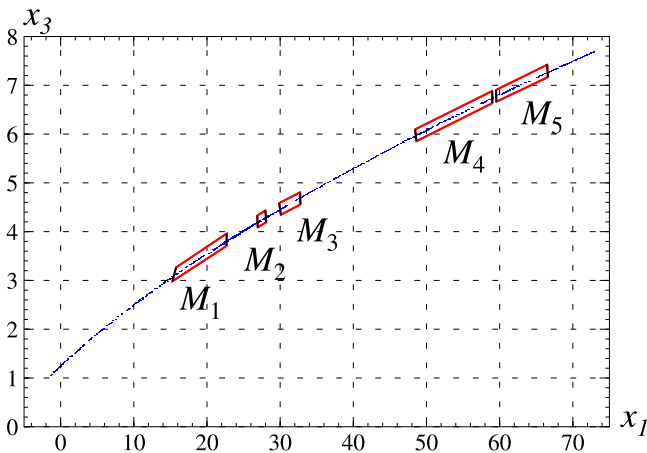


FIG. 6. Symbolic dynamics with five topological rectangles M_i . Vertical edges are plotted in black.

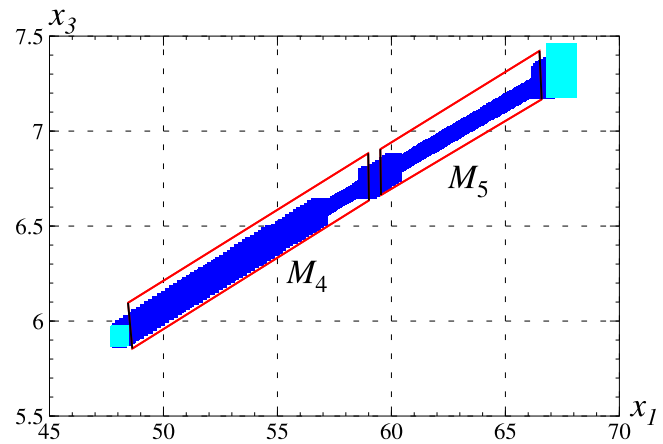


FIG. 7. M_1 P -covers M_4 and M_5 ; vertical and horizontal edges of M_4 and M_5 are plotted in black and red, respectively; enclosures of images of vertical and horizontal edges of M_1 are plotted in cyan and blue, respectively.

in this case a demanding problem. They are constructed using the trial and error method. In fact, we were not able to find less than five sets resulting in a positive topological entropy. The sets M_i are enclosed in the trapping region (compare Fig. 3). It follows that the return map P is well defined on $\bigcup_{i=1}^5 M_i$. Hence, it is sufficient to check the conditions for covering relations for borders of these sets only. It is verified that there are seven covering relations between the sets M_i . For example, M_1 P -covers both M_4 and M_5 . To prove that these covering relations hold the vertical and horizontal edges of M_i and covered by 12 and 395 boxes, respectively. Images of boxes covering vertical and horizontal edges of M_1 are plotted in Fig. 7 in cyan and blue, respectively. One can see that images of the horizontal edges of M_1 do not intersect the horizontal edges of M_4 and M_5 and that images of vertical edges of M_1 are located geometrically on opposite sides of M_4 and M_5 . It follows that M_1 P -covers both M_4 and M_5 . In a similar way, the existence of other covering relations is proved. During the whole proof, the vertical and horizontal edges of M_i are covered by 37 and 1016 boxes, respectively. The proof takes approximately 12 s.

The transition matrix corresponding to covering relations between sets M_i is

$$A_1 = \begin{pmatrix} 0 & 0 & 0 & 1 & 1 \\ 0 & 0 & 1 & 0 & 0 \\ 1 & 0 & 0 & 0 & 0 \\ 1 & 1 & 0 & 0 & 0 \\ 0 & 1 & 0 & 0 & 0 \end{pmatrix}. \tag{5}$$

The dominant eigenvalue of A_1 is $\lambda \approx 1.4142$. It follows that the topological entropy of P can be bounded as

$$h(P) \geq \log(\lambda) > 0.3465. \tag{6}$$

This completes the proof that P is chaotic in the topological sense.

Figure 8 shows topological rectangles N_1, N_2, \dots, N_6 with an improved bound on the topological entropy. The definitions of these

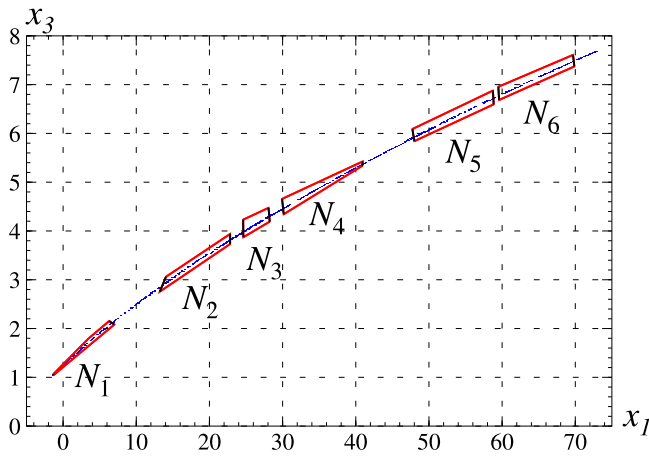


FIG. 8. Symbolic dynamics with six topological rectangles N_i . Vertical edges are plotted in black.

sets are given in the Appendix. Improving the bound on the topological entropy is a challenging research problem. The definitions of the topological rectangles with improved topological entropy have to be very precise. Note that the left-hand side vertical edge of N_1 and the right hand side vertical edge of N_4 are very narrow. For wider edges proving the existence of covering relations involving N_1 and N_4 is not possible. It is verified that there are 10 covering relations between the sets N_i with the following transition matrix:

$$A_2 = \begin{pmatrix} 0 & 0 & 0 & 0 & 1 & 1 \\ 0 & 0 & 0 & 0 & 1 & 1 \\ 0 & 0 & 0 & 1 & 0 & 0 \\ 1 & 1 & 0 & 0 & 0 & 0 \\ 0 & 1 & 1 & 0 & 0 & 0 \\ 0 & 0 & 1 & 0 & 0 & 0 \end{pmatrix}. \tag{7}$$

During the proof, the vertical and horizontal edges of N_i are covered by 89 and 2289 boxes, respectively. The proof takes approximately 24 s. The dominant eigenvalue of A_2 is $\lambda \approx 1.6005$. Hence, we have the following lower bound for the topological entropy of P :

$$h(P) \geq \log(\lambda) > 0.4703. \tag{8}$$

This is a better lower bound than the one given in (6).

The topological entropy $h(\varphi)$ of a continuous time system is defined as the topological entropy of the time one map φ_1 defined as $\varphi_1(x) = \varphi(1, x)$, where $\varphi(t, x)$ denotes the trajectory of the system based at x (see Ref. 23). It follows that one may obtain a lower bound of the topological entropy of the Colpitts oscillator from the lower bound (8) of the topological entropy of the return map, and the upper bound $\tau_{\max} = 13.54$ of the return time for the sets N_1, N_2, \dots, N_6 ,

$$h(\varphi) \geq \frac{h(P)}{\tau_{\max}} > \frac{0.4703}{13.54} > 0.0347. \tag{9}$$

C. Systematic search for periodic orbits

In this section, we study the existence of unstable periodic orbits of the return map P using the combination of the method of close returns, the (standard) Newton method, and the interval Newton method. Non-rigorous estimates of the topological entropy of P based on the number of unstable periodic orbits are calculated.

In order to locate unstable periodic orbits embedded in the attractor, we use the method of close returns.²⁴ In this method a trajectory of a given length N is considered and δ pseudoperiodic orbits with periods $p \leq p_{\max}$ are located. Let us consider a trajectory $(w_i)_{i=1}^N$ of the map P , where $w_{i+1} = P(w_i)$. The sequence $(w_i, w_{i+1}, \dots, w_{i+p-1})$ is called a δ pseudoperiodic orbit with the period p if $\|w_{i+p} - w_i\| \leq \delta$. For each δ pseudoperiodic orbit, we attempt to locate a true period- p orbit in its neighborhood. First, we improve the approximation of a location of a periodic orbit. This is achieved by applying the Newton method to map F defined in (4). The Newton operator

$$N(w) = w - F'(w)^{-1}F(w) \tag{10}$$

is applied iteratively with the initial point being the position of a δ pseudoperiodic orbit. Convergence of the Newton method indicates that a true periodic orbit exists. The elimination procedure based on orbit distance is used to skip periodic orbits found before and to confirm that the minimum period of the periodic orbit found is p . The results obtained for various trajectory lengths N are presented in Table III. During the computations, we use $\delta = 0.1$ and $p_{\max} = 20$.

One can see that the results obtained for $N = 1.8 \times 10^8$ and $N = 2 \times 10^8$ with $p \leq 17$ are the same. One may conclude that there

TABLE III. The number of period- p orbits found using the method of close returns for different lengths N of observed trajectories.

p	$N = 10^7$	$N = 10^8$	$N = 1.8 \times 10^8$	$N = 2 \times 10^8$
1	1	1	1	1
2	1	1	1	1
3	0	0	0	0
4	7	7	7	7
5	0	0	0	0
6	12	12	12	12
7	6	6	6	6
8	36	36	36	36
9	12	12	12	12
10	104	104	104	104
11	50	50	50	50
12	306	306	306	306
13	164	164	164	164
14	937	947	947	947
15	583	598	598	598
16	2532	2926	2927	2927
17	1606	2035	2044	2044
18	5283	9067	9248	9263
19	3358	6753	7047	7077
20	8320	23 807	26 652	27 069
1–20	23 318	46 832	50 162	50 624

is a good chance that all periodic orbits with periods $n \leq 17$ are found. On the other hand, the total number of periodic orbits found when N is increased from 1.8×10^8 to 2×10^8 grows by 462. This means that there are perhaps some periodic orbits with periods $n \geq 18$, which are not found by the search procedure. Locating these orbits would require considering even longer trajectories.

The last step is to prove the existence of periodic orbits found. This is done using the interval Newton operator (2). Let us assume that $\bar{w} = (\bar{w}_1, \bar{w}_2, \dots, \bar{w}_p)$ is an approximate position of the periodic orbit found by applying the standard Newton operator to a δ pseudoperiodic orbit $(w_i, w_{i+1}, \dots, w_{i+p-1})$. We construct an interval vector \mathbf{w} centered at \bar{w} , evaluate the interval Newton operator (2) for map F defined in (4) and verify the existence condition (3). Using this approach, we have successfully proved the existence of all 50 624 periodic orbits reported in Table III. It is verified that all these orbits are unstable.

In this section, we have presented results on the number of periodic orbits obtained by applying the Newton method (both in the standard and interval versions) to the map F defined in (4) and the initial condition $(w_i, w_{i+1}, \dots, w_{i+p-1})$ being the position of a δ pseudoperiodic orbit. An alternative approach is to apply the Newton method to the map $f = P^p - \text{id}$ with the initial condition w_i , where id is the identity map. It is clear that zeros of f are also fixed points of P^p . The usefulness of this approach is confirmed for proving the existence of periodic orbits with periods 1, 2, and 4. For longer orbits, the method usually fails and the proof of existence cannot be carried out. The reason is that the evaluation of f requires the integration of the vector field and its variational equation along the whole orbit. As a result, the matrix $f'(x)^{-1}$ is ill-conditioned and, in consequence, the condition $N(x) \subset x$ usually does not hold. On the other hand, in the case of map F , instead of computing the entire orbit, we calculate short parts of the periodic trajectory only. As a result, rounding errors are smaller, the wrapping effect is reduced, and the procedure enables us to prove the existence of longer periodic orbits.

D. Non-rigorous estimates of the topological entropy

Let us now compare the bound (8) with estimates of the topological entropy based on the number of periodic orbits reported in Table III. Under certain assumptions, the topological entropy of f can be computed as

$$h(f) = \lim_{p \rightarrow \infty} \frac{\log(C_p)}{p}, \tag{11}$$

where C_p denotes the number of fixed points of f^p (compare Ref. 19). Hence, the expression

$$h_p = \frac{\log(C_p)}{p} \tag{12}$$

for a large p is frequently used as an estimate of $h(f)$. The results obtained by applying this formula to the results presented in the last column of Table III are plotted in Fig. 9 using red circle symbols. One can see that for $p \geq 14$, the estimates h_p oscillate between 0.6 and 0.7. For comparison, we also plot the results obtained by applying the formula (12) to the number of fixed points of P^p based on the existence of symbolic dynamics with the transition matrix (7).

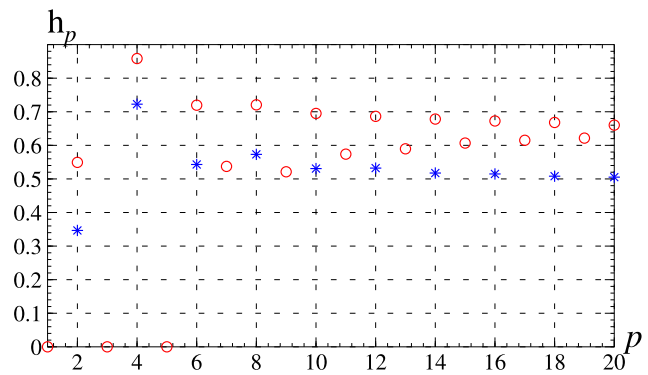


FIG. 9. Estimates $h_p = p^{-1} \log(C_p)$ of the topological entropy of P based on the number C_p of fixed points of P^p ; the results based on the number of periodic orbits found are plotted as red circles; the results based on the existence of symbolic dynamics with the transition matrix (7) are plotted as blue stars.

The number of fixed points of P^p supported by covering relations with the transition matrix A can be computed as the trace (the sum of the diagonal elements) of A^p . One can see that there are no periodic orbits with odd periods supported by the existence of symbolic dynamics. Moreover, for even periods, the estimates based on the existence of symbolic dynamics are much lower than the ones based on the number of periodic orbits found. It follows that the symbolic dynamics with the transition matrix (7) does not capture the whole topological complexity of P . Finding a better lower bound of the topological entropy of P is a subject of future research.

Let us now estimate the topological entropy of the flow (1). Under certain assumptions, the topological entropy of a continuous time system can be estimated based on short periodic orbits using the following formula:²⁵

$$h(\varphi) = \lim_{t \rightarrow \infty} \frac{\log(C_t)}{t}, \tag{13}$$

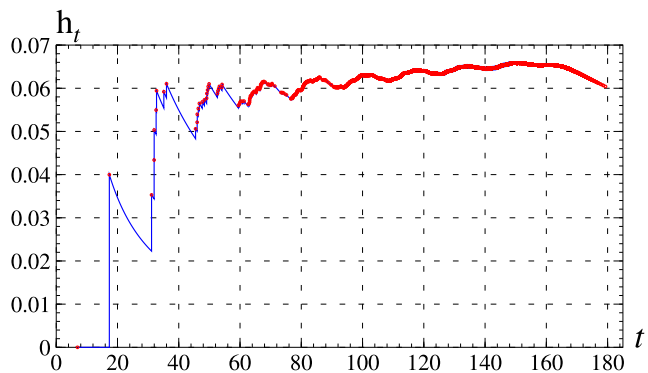


FIG. 10. Estimates $h_t = t^{-1} \log(C_t)$ of the topological entropy of the flow (1) based on periodic orbits found.

where C_t is the number of periodic orbits with the flow time smaller or equal to t . Estimates $h_t = t^{-1} \log(C_t)$ obtained using the results presented in Table III are plotted in Fig. 10. Points at which estimates grow due to the existence of a periodic orbit with a given flow time are depicted as red dots.

In the region $t \in [100, 160]$, the estimates oscillate in the interval $[0.06, 0.07]$. A drop of estimates in the region $t > 160$ is caused by the fact that the search for periodic orbits of P is limited to cycles with periods $p \leq 20$, while some cycles with periods $p > 20$ have flow times in the interval $[160, 180]$. Let us also note that estimates presented in Fig. 10 are considerably larger than the lower bound (9). This observation confirms the statement that the complexity of the Colpitts oscillator is higher than the one revealed by the existence of covering relations with the transition matrix (7).

V. CONCLUSIONS

A numerical study of the Colpitts oscillator was carried out. It was shown that the circuit displays rich dynamical behaviors. The existence of periodic attractors was proved using the interval Newton method. For the chaotic case, a trapping region for the associated return map was constructed and the existence of at least one attractor that belongs to this set was proved. Using the method of covering relations, it was proved that the Colpitts oscillator is chaotic in the topological sense. Positive lower bounds on the topological entropy of the return map and of the flow were found. Using the combination of interval arithmetic tools and the method of close returns, the existence of several thousands of periodic orbits embedded in the chaotic attractor was proved and accurate approximations of the true value of the topological entropy of the system were calculated.

ACKNOWLEDGMENTS

This work was supported in part by the AGH University of Science and Technology, Kraków, Poland. The author acknowledges the collaboration with Mr. Marcin Flis on the results presented in this manuscript during Mr. Flis enrollment in the AGH Doctoral School.

AUTHOR DECLARATIONS

Conflict of Interest

The authors have no conflicts to disclose.

Author Contributions

Zbigniew Galias: Investigation (equal); Software (equal); Visualization (equal); Writing – original draft (equal); Writing – review & editing (equal).

DATA AVAILABILITY

The data that support the findings of this study are available from the corresponding author upon reasonable request.

APPENDIX A: DEFINITIONS OF POLYGONS T , M_i , N_i

Definition of the trapping region T :

$$T = ((-1.89, 2, 0.88), (-2.51, 2, 1.16), (13.38, 2, 2.97), (34.12, 2, 5.06), (74.24, 2, 7.93), (74.49, 2, 7.61), (43.91, 2, 5.47), (15.92, 2, 2.97), (-1.89, 2, 0.88)).$$

Definitions of five topological rectangles M_i with complex symbolic dynamics:

$$\begin{aligned} M_1 &= ((15.275\ 30, 2, 2.982\ 78), (15.774\ 10, 2, 3.266\ 45), \\ &\quad (17.504\ 29, 2, 3.440\ 20), (20.964\ 68, 2, 3.787\ 70), \\ &\quad (22.694\ 87, 2, 3.961\ 45), (22.663\ 70, 2, 3.706\ 14)), \\ M_2 &= ((26.934\ 62, 2, 4.089\ 10), (26.872\ 27, 2, 4.330\ 22), \\ &\quad (27.426\ 02, 2, 4.382\ 18), (27.979\ 76, 2, 4.434\ 13), \\ &\quad (28.106\ 58, 2, 4.193\ 13)), \\ M_3 &= ((30.093\ 30, 2, 4.344\ 08), (29.865\ 04, 2, 4.585\ 52), \\ &\quad (31.299\ 07, 2, 4.695\ 45), (32.733\ 11, 2, 4.805\ 37), \\ &\quad (32.764\ 28, 2, 4.557\ 16)), \\ M_4 &= ((48.632\ 17, 2, 5.854\ 95), (48.445\ 13, 2, 6.096\ 07), \\ &\quad (51.079\ 38, 2, 6.292\ 87), (56.347\ 90, 2, 6.686\ 46), \\ &\quad (58.982\ 16, 2, 6.883\ 26), (59.013\ 33, 2, 6.635\ 05)), \\ M_5 &= ((59.543\ 30, 2, 6.663\ 42), (59.512\ 13, 2, 6.904\ 54), \\ &\quad (64.749\ 47, 2, 7.292\ 81), (66.495\ 25, 2, 7.422\ 24), \\ &\quad (66.588\ 77, 2, 7.166\ 93)). \end{aligned}$$

Definitions of six topological rectangles N_i with complex symbolic dynamics:

$$\begin{aligned} N_1 &= ((-1.248\ 25, 2, 1.051\ 59), (-1.313\ 14, 2, 1.06\ 756), \\ &\quad (3.462\ 33, 2, 1.792\ 89), (6.301\ 39, 2, 2.153\ 71), \\ &\quad (6.999\ 16, 2, 2.081\ 50)), \\ N_2 &= ((13.217\ 42, 2, 2.756\ 67), (22.824\ 77, 2, 3.731\ 92), \\ &\quad (22.827\ 79, 2, 3.938\ 76), (14.059\ 35, 2, 3.060\ 63)), \\ N_3 &= ((24.611\ 87, 2, 4.231\ 47), (28.077\ 69, 2, 4.473\ 97), \\ &\quad (28.236\ 79, 2, 4.191\ 76), (24.632\ 65, 2, 3.871\ 21)), \\ N_4 &= ((29.924\ 74, 2, 4.656\ 75), (40.950\ 65, 2, 5.425\ 33), \\ &\quad (40.882\ 03, 2, 5.335\ 00), (30.149\ 51, 2, 4.343\ 08)), \\ N_5 &= ((47.736\ 74, 2, 6.089\ 05), (58.743\ 50, 2, 6.877\ 11), \\ &\quad (58.846\ 18, 2, 6.595\ 66), (48.003\ 70, 2, 5.841\ 37)), \\ N_6 &= ((59.482\ 76, 2, 6.955\ 92), (69.688\ 65, 2, 7.608\ 89), \\ &\quad (69.873\ 47, 2, 7.372\ 47), (59.585\ 43, 2, 6.685\ 73)). \end{aligned}$$

REFERENCES

- ¹L. O. Chua, M. Komuro, and T. Matsumoto, "The double scroll family," *IEEE Trans. Circuits Syst.* **33**, 1037–1118 (1986).
- ²M. P. Kennedy, "Chaos in the Colpitts oscillator," *IEEE Trans. Circuits Syst. I* **41**, 771–774 (1994).
- ³G. Maggio, O. De Feo, and M. Kennedy, "Nonlinear analysis of the Colpitts oscillator and applications to design," *IEEE Trans. Circuits Syst. I* **46**, 1118–1130 (1999).
- ⁴G. M. Maggio, M. di Bernardo, and M. P. Kennedy, "Nonsmooth bifurcations in a piecewise-linear model of the Colpitts oscillator," *IEEE Trans. Circuits Syst.* **47**, 1160–1177 (2000).
- ⁵I. M. Filanovsky, C. J. M. Verhoeven, and M. Reja, "Remarks on analysis, design and amplitude stability of MOS Colpitts oscillator," *IEEE Trans. Circuits Syst. II* **54**, 800–804 (2007).
- ⁶S. Rasappan and N. K. Jothi, "Control of Colpitts-oscillator via adaptive nonlinear control," in *2014 International Conference on Science Engineering and Management Research (ICSEMR)* (IEEE, 2014), pp. 1–5.
- ⁷A. Semenov, K. Koval, A. Savitskiy, O. Zviahin, and S. Baraban, "Numerical study of the deterministic chaos oscillator with a differential integral element on the Colpitts circuit," in *2018 14th International Conference on Advanced Trends in Radioelectronics, Telecommunications and Computer Engineering (TCSET)* (IEEE, 2018), pp. 846–850.
- ⁸Z. Galias, C. A. Murphy, M. P. Kennedy, and M. J. Ogorzalek, "Electronic chaos controller," *Chaos Soliton. Fract.* **8**, 1471–1484 (1997).
- ⁹A. Tamasevicius, G. Mykolaitis, S. Bumeliene, A. Baziliauskas, R. Krivickas, and E. Lindberg, "Chaotic Colpitts oscillator for the ultrahigh frequency range," *Nonlinear Dyn.* **44**, 159–165 (2006).
- ¹⁰J. Kengne, J. C. Chedjou, G. Kenné, and K. Kyamakya, "Dynamical properties and chaos synchronization of improved Colpitts oscillators," *Commun. Nonlinear Sci. Numer. Simul.* **17**, 2914–2923 (2012).
- ¹¹R. Tchitnga, T. Nguazon, P. H. Louodop Fotso, and J. A. C. Gallas, "Chaos in a single op-amp-based jerk circuit: Experiments and simulations," *IEEE Trans. Circuits Syst. II* **63**, 239–243 (2016).
- ¹²M. Abdullah, S. Iqbal, and U. Shahid, "On the study of chaotic Colpitts oscillator using simulations and experiments," in *2018 International Conference on Electrical Engineering (ICEE)* (IEEE, 2018), pp. 1–6.
- ¹³F. Behzad and M. Hamdipour, "Detailed investigation of chaos in a Colpitts oscillator," *Pramana—J. Phys.* **95**, 2 (2021).
- ¹⁴I. Vasiljević, A. Lekić, and D. Stipanović, "Lyapunov analysis of the chaotic Colpitts oscillator," in *2019 IEEE International Symposium on Circuits and Systems (ISCAS)* (IEEE, 2019), pp. 1–5.
- ¹⁵A. Neumaier, *Interval Methods for Systems of Equations* (Cambridge University Press, Cambridge, 1990).
- ¹⁶W. Tucker, *Validated Numerics: A Short Introduction to Rigorous Computations* (Princeton University Press, 2011).
- ¹⁷T. Kapela, M. Mrozek, D. Wilczak, and P. Zgliczyński, "CAPD::DynSys: A flexible C++ toolbox for rigorous numerical analysis of dynamical systems," *Commun. Nonlinear Sci. Numer. Simul.* **101**, 105578 (2020).
- ¹⁸A. Wolf, J. B. Swift, H. L. Swinney, and J. A. Vastano, "Determining Lyapunov exponents from a time series," *Physica D* **16**, 285–317 (1985).
- ¹⁹C. Robinson, *Dynamical Systems: Stability, Symbolic Dynamics, and Chaos* (CRC Press, Boca Raton, FL, 1995).
- ²⁰P. Zgliczyński, "Computer assisted proof of chaos in the Rössler equations and in the Hénon map," *Nonlinearity* **10**, 243–252 (1997).
- ²¹P. Zgliczyński, "Covering relations, cone conditions and the stable manifold theorem," *J. Differ. Equ.* **246**, 1774–1819 (2009).
- ²²Z. Galias, "The dangers of rounding errors for simulations and analysis of nonlinear circuits and systems—And how to avoid them," *IEEE Circuits Syst. Mag.* **13**, 35–52 (2013).
- ²³I. Cornfeld, S. Fomin, and Y. Sinai, *Ergodic Theory* (Springer Verlag, New York, 1982).
- ²⁴D. Lathrop and E. Kostelich, "Characterisation of an experimental strange attractor by periodic orbits," *Phys. Rev. A* **40**, 4028–4031 (1989).
- ²⁵R. Bowen, "Periodic points and measures for axiom A diffeomorphisms," *Trans. Am. Math. Soc.* **154**, 377–397 (1971).